An activating *Pik3ca* mutation coupled with *Pten* loss is sufficient to initiate ovarian tumorigenesis in mice

Kathryn M. Kinross,[1] Karen G. Montgomery,[1] Margarete Kleinschmidt,[1] Paul Waring,[2] Ivan Ivetac,[1] Anjali Tikoo,[1] Mirette Saad,[1,3] Lauren Hare,[1,4] Vincent Roh,[1] Theo Mantamadiotis,[2] Karen E. Sheppard,[1,3] Georgina L. Ryland,[1,5] Ian G. Campbell,[1,2] Kylie L. Gorringe,[1,2] James G. Christensen,[6] Carleen Cullinane,[1,2] Rodney J. Hicks,[1,7,8] Richard B. Pearson,[1,3,4] Ricky W. Johnstone,[1,2] Grant A. McArthur,[1,2,7,9] and Wayne A. Phillips[1,4,10,11]

[1]Cancer Research Division, Peter MacCallum Cancer Centre (Peter Mac), East Melbourne, Victoria, Australia. [2]Pathology Department and [3]Biochemistry and Molecular Biology Department, University of Melbourne, Melbourne, Victoria, Australia. [4]Biochemistry and Molecular Biology Department and [5]Monash Institute of Medical Research, Monash University, Clayton, Victoria, Australia. [6]Pfizer Global Research and Development, La Jolla, California, USA. [7]Department of Medicine, St. Vincent's Hospital, University of Melbourne, Melbourne, Victoria, Australia. [8]Centre for Cancer Imaging, [9]Cancer Medicine Division and [10]Cancer Surgery Division, Peter Mac, East Melbourne, Victoria, Australia. [11]Department of Surgery, St. Vincent's Hospital, University of Melbourne, Melbourne, Victoria, Australia.

Mutations in the gene encoding the p110α subunit of PI3K (*PIK3CA*) that result in enhanced PI3K activity are frequently observed in human cancers. To better understand the role of mutant *PIK3CA* in the initiation or progression of tumorigenesis, we generated mice in which a *PIK3CA* mutation commonly detected in human cancers (the H1047R mutation) could be conditionally knocked into the endogenous *Pik3ca* locus. Activation of this mutation in the mouse ovary revealed that alone, $Pik3ca^{H1047R}$ induced premalignant hyperplasia of the ovarian surface epithelium but no tumors. Concomitantly, we analyzed several human ovarian cancers and found *PIK3CA* mutations coexistent with *KRAS* and/or *PTEN* mutations, raising the possibility that a secondary defect in a co-regulator of PI3K activity may be required for mutant *PIK3CA* to promote transformation. Consistent with this notion, we found that $Pik3ca^{H1047R}$ mutation plus *Pten* deletion in the mouse ovary led to the development of ovarian serous adenocarcinomas and granulosa cell tumors. Both mutational events were required for early, robust Akt activation. Pharmacological inhibition of PI3K/mTOR in these mice delayed tumor growth and prolonged survival. These results demonstrate that the $Pik3ca^{H1047R}$ mutation with loss of *Pten* is enough to promote ovarian cell transformation and that we have developed a model system for studying possible therapies.

Introduction

In human cancers, somatic mutations in *PIK3CA* commonly target specific hot spots in the helical (E542 and E545) and kinase (H1047) domains (1, 2), resulting in enhanced lipid kinase activity and upregulation of downstream signaling events such as phosphorylation of Akt (3). Activation of Akt is observed in up to 70% of ovarian cancers (4) due to a variety of causes, including *PIK3CA* mutations (8%–12%) or amplification (3%–8%) and/or PTEN loss (27%) or mutations (3–8%) (1, 5–10). Loss of *Pten* (11, 12) or overexpression of activated *PI3K* in the mouse ovarian surface epithelium (OSE) (13) do not lead to tumor formation; however, the ability of mutant *Pik3ca* to initiate tumorigenesis or drive tumor progression has not been established. Here we describe an animal model that allows us to study the effects of the $Pik3ca^{H1047R}$ mutation in the physiologically relevant context of a somatic, heterozygous *Pik3ca* mutation expressed at endogenous levels in otherwise normal cells and tissues.

Results and Discussion

We analyzed 87 human ovarian cancers for changes in PI3K pathway genes *PIK3CA*, *PIK3R1* (encoding the PI3K p85 regulatory subunit), *PTEN*, and also in *KRAS*, which interacts with PI3K to mediate its activity (refs. 14, 15, and Supplemental Table 1; supplemental material available online with this article; doi:10.1172/JCI59309DS1). We found 37% of samples exhibited genetic aberrations in one of these genes. Notably, 4 (40%) of the 10 patients who had *PIK3CA* mutations also exhibited *PIK3R1*, *PTEN*, and/or *KRAS* mutations. Analysis of 34 ovarian cancer cell lines found 3 (*IGROv1*, *TOV21G*, and *MCAS*) had coexisting *PIK3CA* mutation with *PTEN* and/or *KRAS* aberrations (Supplemental Table 1). Consistent with this, studies in endometrioid ovarian (11), breast, endometrial, and colon cancers (16) have identified tumors with coexistent *PIK3CA* and *PTEN* mutations. Neither the role of endogenous levels of mutant *PIK3CA* nor the cooperative nature of *PIK3CA* and *PTEN* mutations has been evaluated in vivo.

To address this, we used what we believe to be a novel exon-switch strategy to generate a mutant mouse harboring a germline *Pik3ca* allele with a conditional H1047R mutation. We inserted loxP sites flanking exon 20 of *Pik3ca* and downstream placed a tandem copy of exon 20 containing a CAT→AGG change in codon 1047 (Figure 1A and Supplemental Figures 1 and 2). Adenoviral Cre–mediated (AdCre-mediated) recombination leads to replacement of wild-type with mutant exon 20, resulting in p110α-H1047R protein expression at endogenous levels in otherwise normal cells, thus accurately reproducing the scenario of a naturally occurring muta-

Conflict of interest: James G. Christensen is a Pfizer employee and shareholder.
Citation for this article: *J Clin Invest.* 2012;122(2):553–557. doi:10.1172/JCI59309.

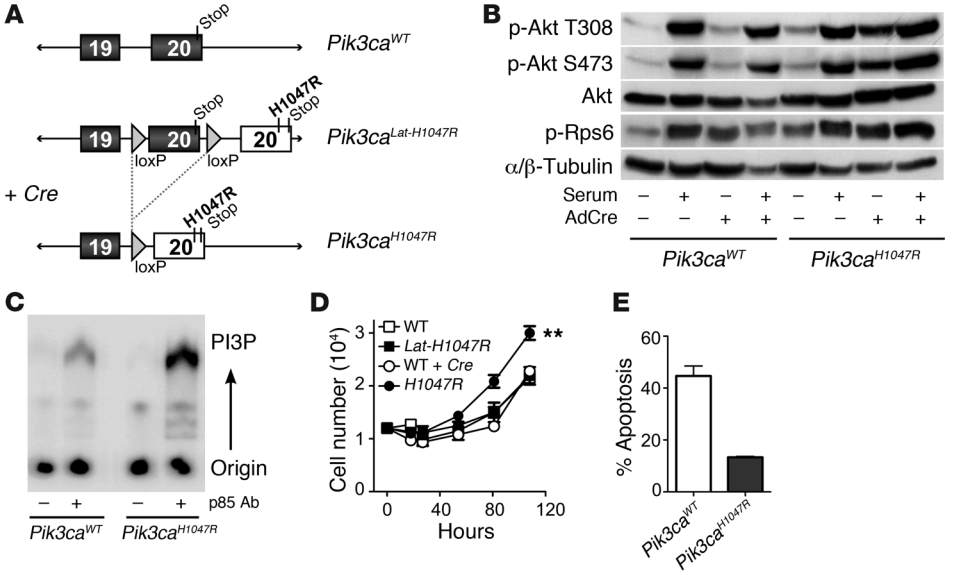

Figure 1

Pik3ca^{H1047R} results in increased PI3K activity and functional changes in MEFs. (**A**) Schematic of the conditional *Pik3ca*^{H1047R} allele. (**B**) Protein blot in AdCre-treated (+) and untreated (–) *Pik3ca*^{WT} and *Pik3ca*^{H1047R} MEFs with (+) and without (–) 5-minute serum stimulation. (**C**) MEFs from *Pik3ca*^{WT} or *Pik3ca*$^{Lat\text{-}H1047R}$ mice were infected with AdCre, and PI3K was immunoprecipitated using an anti-p85 antibody. PI3K activity in the immunoprecipitates was assayed using phosphatidylinositol (PI) as substrate. Phosphorylated lipids were separated by thin-layer chromatography and visualized by phosphoimager. (**D**) MEFs from *Pik3ca*^{WT} and *Pik3ca*^{H1047R} mice before or after AdCre infection were cultured and cells counted (**$P < 0.05$ versus WT). (**E**) Apoptosis was assessed using annexin V after 72 hours serum deprivation. Results are mean ± SEM; 3 independent MEF preparations.

tion. The presence of the conditional allele did not affect development (Supplemental Table 2). Using murine embryonic fibroblasts (MEFs), we confirmed the knock-in of the *Pik3ca*^{H1047R} mutation after AdCre infection in vitro (Supplemental Figures 3 and 4). *Pik3ca*^{H1047R} resulted in elevated p-Akt and p–ribosomal protein S6 (p-Rps6) levels, increased PI3K activity, enhanced proliferation, and reduced apoptosis (Figure 1, B–E). We have thus generated a model system in which the biological effects of *Pik3ca*^{H1047R} expression can be examined both in vivo and in vitro.

Combining this mouse with a Cre-inducible knockout of *Pten* (17), we investigated whether two genetic hits affecting PI3K regulation (*Pik3ca*^{H1047R} and *Pten* loss) are sufficient to promote tumorigenesis in the ovary. We induced the *Pik3ca*^{H1047R} mutation and/or deleted *Pten* in the left ovary by intrabursal AdCre delivery, which targets recombination to the OSE, granulosa cells of the ovarian follicles, and ovarian bursal cells (refs. 11, 12, 18, 19, and Supplemental Figure 5).

At 8 weeks after AdCre infection, OSE of *Pik3ca*^{H1047R} mice showed mild, focal papillary serous hyperplasia, and *Pik3ca*^{H1047R}*Pten*$^{del/del}$ mice showed marked hyperplasia (Figure 2A). p-Akt T308 and p-Akt S473 staining was strongest and located at the membrane in the OSE of double *Pik3ca*^{H1047R}*Pten*$^{del/del}$ mutants (Figure 2A).

Over 1 year of observation, no wild-type or single mutant mice developed tumors. *Pik3ca*^{H1047R}, *Pik3ca*^{H1047R}*Pten*$^{del/WT}$, and *Pten*$^{del/del}$ mice developed serous papillary hyperplasia of the OSE (Figure 2B, Supplemental Figure 6, and Table 1), coincident with an increase in p-Akt T308 and p-Akt S473 compared with equivalent OSE at 8 weeks after AdCre infection. The degree of the hyperplasia varied between mice and was highest in the *Pik3ca*^{H1047R} and *Pik3ca*^{H1047R}*Pten*$^{del/WT}$ compared with the *Pten*$^{del/del}$ mice, suggesting that alone, *Pik3ca*^{H1047R} more potently promotes proliferative changes compared with *Pten* loss. In some *Pik3ca*^{H1047R} mice, the hyperplasia resembled epithelial proliferation seen in the borderline (low malignant potential) subtype of human ovarian serous carcinoma. In 2 mice, we observed microinvasion of the ovarian stroma, indicating that the epithelial proliferation was neoplastic despite the absence of definitive cytological evidence of malignancy. The inability of *Pik3ca*^{H1047R} to induce ovarian tumorigenesis differs from transgenic mouse models of *Pik3ca*^{H1047R} inducing lung and breast (20–23) tumors, but these models are driven by overexpressed *Pik3ca*^{H1047R} rather than mutation of the endogenous gene, as occurs in human tumors. Possibly, the ovary could be less susceptible to transformation via a single mutation compared with other tissue types. Studies are underway to examine the role of this mutation in the lung, breast, and gastrointestinal tract.

In contrast to the single mutant mice, all *Pik3ca*^{H1047R}*Pten*$^{del/del}$ mice developed ovarian masses, necessitating sacrifice with a median latency of 16 weeks (Figure 2B and Figure 3, A and B). Macroscopic analyses at autopsy revealed that many *Pik3ca*^{H1047R} *Pten*$^{del/del}$ mice developed hemorrhagic ascites, and some showed intraperitoneal masses on the peritoneal wall and diaphragm. No distant metastases were evident macroscopically. Histological examination confirmed malignancy in 15 of 18 ovarian masses, consisting of ovarian serous adenocarcinomas (Figure 3, D and E), ovarian granulosa cell tumors (Figure 3, I–K), and a single ovarian luteoma (Table 1). Three mice had collision tumors composed of different histological cancer types within the same mass. Serous carcinomas exhibited high abundance and membrane localization of p-Akt S473, p-Akt T308 (Figure 2B and Figure 3F), cytoplasmic p-Rps6 (Figure 3G), and keratin (Figure 3H). Granulosa cell tumors were positive for inhibin (Figure 3K). Expression of the *Pik3ca*^{H1047R} mutant and loss of PTEN protein were confirmed in tumors (Figure 2 and Supplemental Figure 7). Consistent with these findings, recent genomic analysis of high-grade serous ovarian cancers shows that while PIK3CA amplification and mutations are rare events in this subtype, upregulation of the pathway is seen in 45% of cases (24).

Additionally, 13 of the 15 (86.7%) *Pik3ca*^{H1047R}*Pten*$^{del/del}$ mice showed variable degrees of fibrous and/or smooth muscle hyperplasia, which formed irregular or solid masses of desmoplastic stroma or resulted in bursal wall thickening by actin-positive smooth muscle (data not shown). This phenotypic heterogeneity demonstrates that combined *Pik3ca*^{H1047R} mutation and *Pten* loss

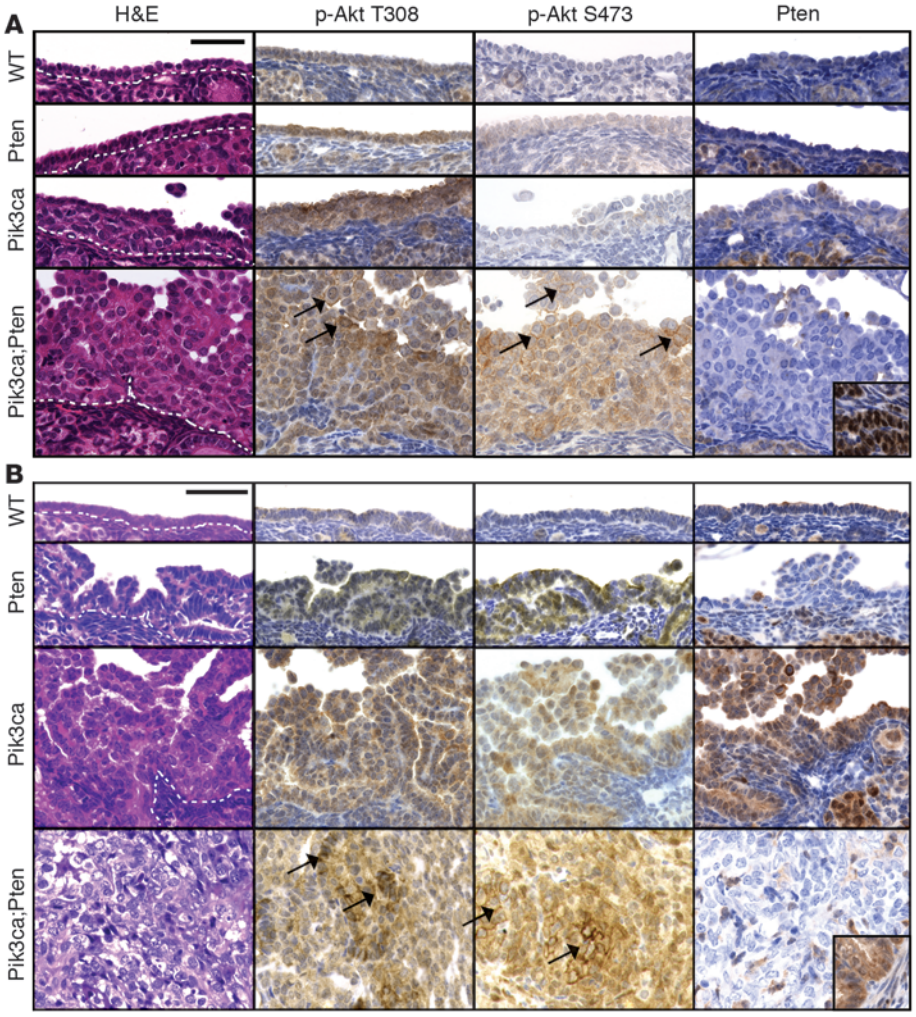

Figure 2
Pik3ca^{H1047R} and *Pten* deletion leads to robust p-Akt T308 and p-Akt S473 levels in OSE. Representative histological images of OSE from *Pik3ca*^{WT}*Pten*^{WT} (WT, n = 6), *Pik3ca*^{WT}*Pten*$^{del/del}$ (Pten, n = 6), *Pik3ca*^{H1047R}*Pten*^{WT} (Pik3ca, n = 6), *Pik3ca*^{H1047R}*Pten*$^{del/del}$ (Pik3ca; Pten, n = 5) mice at (**A**) 8 weeks and (**B**) 12 months after AdCre infection (except for *Pik3ca*^{H1047R}*Pten*$^{del/del}$, taken at 6 months); H&E and IHC staining. Dotted lines show the intersection of the OSE and stromal layer. Arrows indicate membranous p-Akt localization. Scale bars: 50 μm. Insets are positively stained area of WT tissue on same section.

can cooperate to potently promote proliferation or transformation in several cell types, including OSE, ovarian granulosa cells, fibroblasts, and smooth muscle cells following AdCre infection.

We compared PI3K/Akt/mTOR pathway signaling in *Pik3ca*^{H1047R}*Pten*$^{del/del}$ tumor lysates with that in other mouse ovarian cancer models: *Kras*^{G12D}*Pten*$^{del/del}$ and *Apc*$^{S580/S580}$*Pten*$^{del/del}$ (refs. 11, 12, and Figure 3L). *Pik3ca*^{H1047R}*Pten*$^{del/del}$ and *Kras*^{G12D}*Pten*$^{del/del}$ tumors exhibited equivalent pathway signaling to multiple substrate proteins. While *Apc*$^{S580/S580}$*Pten*$^{del/del}$ tumors showed equivalent p-Pdk1 and p-Rps6 levels, they showed relatively low levels of p-Akt and its substrates. This suggests that cooperating mutations — *Pten* loss and *Kras* or *Pik3ca* mutation, but not *Apc* mutation — are required to robustly activate Akt and its direct targets.

These mutations may cooperate because both *Pik3ca*^{H1047R} kinase activity and loss of PTEN's phosphatase activity are necessary to reach a threshold of PIP_3 levels required for transformation. Alternatively, since PTEN has additional, PI3K-independent tumor-suppressive functions (25), its loss may promote tumorigenesis via these additional mechanisms. Finally, both mutations may be required to overcome negative feedback loops that could be activated as a result of only one of these genetic events.

To examine whether established *Pik3ca*^{H1047R}*Pten*$^{del/del}$ tumors remained dependant on PI3K pathway activity for tumor maintenance, we utilized an ATP-competitive PI3K/mTOR inhibitor, PF04691502, currently in phase I clinical trials (26, 27). Treatment of *Pik3ca*^{H1047R}*Pten*$^{del/del}$ mice commenced 10 weeks following AdCre exposure (Figure 3M), and tumor progression was monitored by ultrasound (Supplemental Figure 8). Early response was characterized by cytostasis, which significantly lengthened median survival time (Figure 3M), indicating a continued dependence on PI3K and/or mTOR for tumorigenesis in this model. Interestingly, tumors eventually regrew despite continuous PI3K/mTOR inhibition with PF04691502. This suggests that patients with *PIK3CA*^{H1047R} mutations and loss of *PTEN* could be initially responsive to PI3K/mTOR inhibition, but that resistance is likely to develop. This model has the potential to provide a crucial new system for examining resistance mechanisms to PI3K pathway inhibitors and for testing novel therapeutics targeting the PI3K pathway alone or in combination with other therapies.

In summary, study of the *Pik3ca*^{H1047R} mouse model described herein has demonstrated that *Pik3ca* mutation requires a second hit to initiate tumorigenesis in the ovary. We found that mutations in PI3K regulatory proteins co-occur in human ovarian tumors with *PIK3CA* mutations and demonstrate that in vivo, *Pik3ca*^{H1047R} and loss of *Pten* is sufficient to promote ovarian cell transformation.

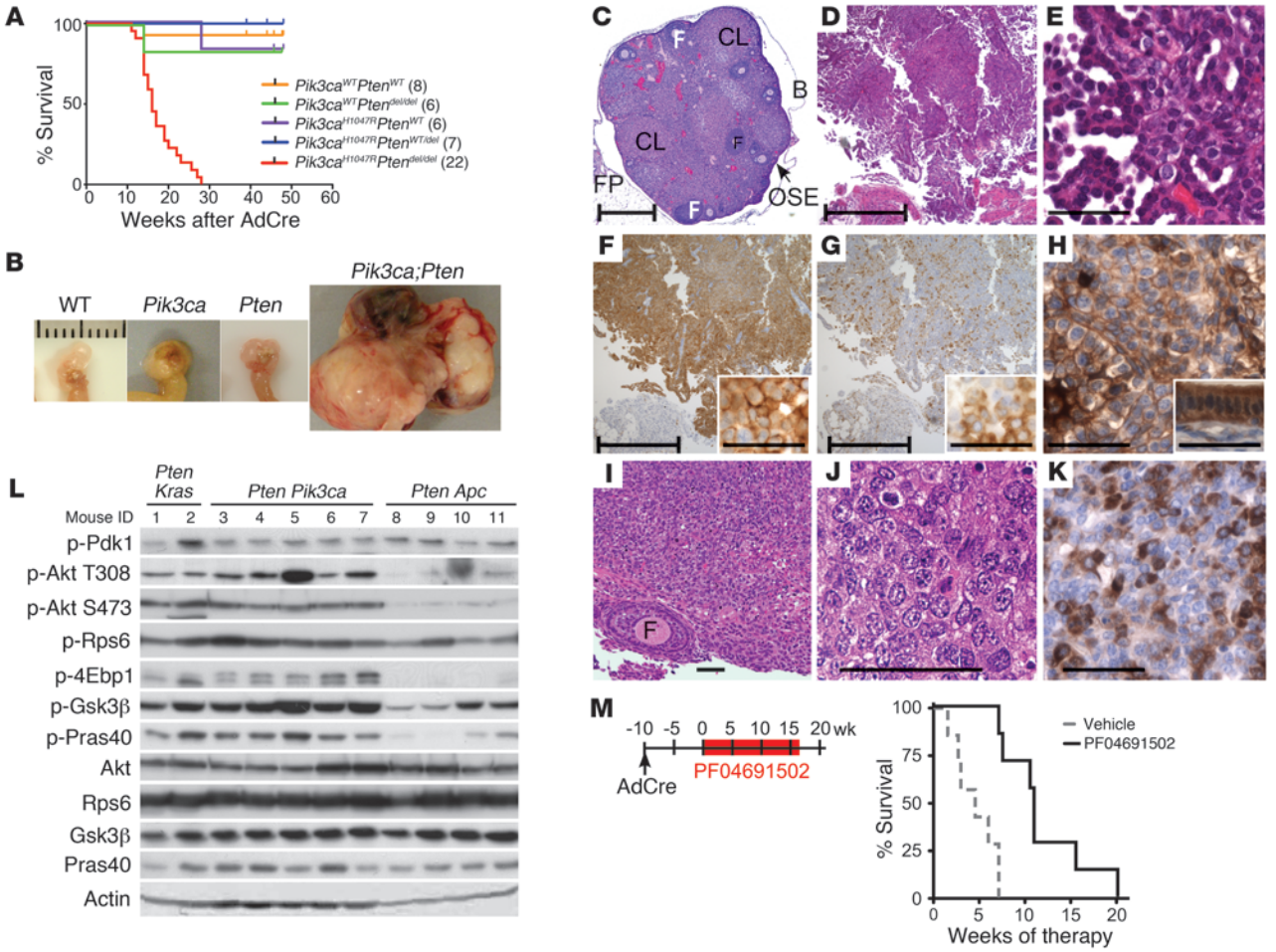

Figure 3

Pik3ca^{H1047R} and *Pten*$^{del/del}$ cooperate to promote tumorigenesis in mouse ovary. (**A**) Kaplan-Meier curve of *Pik3ca*^{H1047R}*Pten*$^{del/del}$ mice (red; median survival, 16 weeks) compared with control mice (*n* in parentheses) exposed to AdCre in the ovarian bursa. (**B**) Ovarian tumors from *Pik3ca*^{H1047R}*Pten*$^{del/del}$ mice (20–25 weeks after AdCre infection) and non-tumor-bearing control mice 1 year after AdCre infection. Scale bars: 1 cm. (**C**–**K**) Representative histopathology of tumors from *Pik3ca*^{H1047R}*Pten*$^{del/del}$ mice. Non-AdCre-exposed ovary (**C**), serous adenocarcinoma (**D**–**H**), and granulosa cell tumor (**I**–**K**). Staining with H&E (**C**–**E**, **I**, and **J**), p-Akt S473 (**F**, high-power inset), p-Rps6 (**G**, high power inset), pan-keratin (**H**, adjacent uterus inset), or inhibin (**K**) is shown. Scale bars: bracketed, 500 mm; unbracketed, 50 mm. B, bursa; CL, corpus luteum; F, follicle; FP, fat pad. (**L**) Protein blots from *Kras*^{G12D}*Pten*$^{del/del}$ (*Pten Kras*), *Pik3ca*^{H1047R}*Pten*$^{del/del}$ (*Pten Pik3ca*), and *Apc*$^{S580/S580}$*Pten*$^{del/del}$ (*Pten Apc*) ovarian tumors. (**M**) Tumor-bearing *Pik3ca*^{H1047R}*Pten*$^{del/del}$ mice were treated with vehicle or PF04691502 daily. Mice receiving vehicle exhibited 4.5 weeks median survival compared with 11 weeks in PF04691502-treated mice; log-rank (Mantel-Cox) test, $P = 0.0006$.

Methods

Generation of Pik3ca$^{Lat\text{-}H1047R}$ *mice*. *Pik3ca*$^{Lat\text{-}H1047R}$ mice were generated by homologous recombination in embryonic stem cells (Ozgene). The targeting construct, detailed in Supplemental Figure 1, was assembled from C57BL/6 genomic DNA and cloned into the Ozgene F_PacI_Neo vector containing a PGK-neomycin cassette flanked by FLP recombinase target (FRT) sequences. The targeting vector was electroporated into 129S1/Sv-derived W9.5 ES cells. Targeted ES cells were injected into C57BL/6 blastocysts and chimeras crossed with C57BL/6 mice. The PGK-neomycin cassette was deleted by crossing with C57BL/6 ACTB-FLPe mice.

AdCre recombination in the ovary. Cells in the ovarian bursa were infected with AdCre, a gift from Walter Thomas (Baker IDI Heart and Diabetes Institute, Melbourne, Victoria, Australia) as described previously (18); details are provided in Supplemental Methods. Endpoints were excessive tumor burden (>1.5 cm^3), severe abdominal distension, or signs of severe illness (hunching, ruffled fur, or loss of responsiveness).

Mouse cohorts. *Pten*$^{del/del}$ mice (c;129S4-Pten^{tm1Hwu}/J) were from The Jackson Laboratory. All *Pik3ca*^{H1047R}*Pten*$^{del/del}$ mice were maintained on a mixed (C57BL/6; BALB/c; 129S4) background, and littermates were used where possible. *Pik3ca*^{H1047R} refers to heterozygotes. *Kras*^{G12D} *Pten*$^{del/del}$ and *APC*$^{580S/580S}$*Pten*$^{del/del}$ ovarian tumor samples were generated using *APC*^{580S} (a gift from Tetsuo Noda, Department of Cell Biology, Cancer Institute, Toshima-ku, Tokyo, Japan; ref. 28) and *Kras*^{G12D} (MMHCC, ref. 29) mice.

Histology and protein analysis. Tumors were formalin fixed, and immunohistochemistry was performed as described previously (27). For Western blotting, tumors were snap frozen and lysed in RIPA buffer. Antibodies are detailed in Supplemental Methods.

In vivo therapy. Mice received vehicle (0.5% methylcellulose) or 10 mg/kg PF04691502 orally, daily. Ovary volume was monitored by ultrasound imaging (Vevo 770, Visualsonics). Endpoints were as above or weight loss of greater than 20%.

Table 1

Pik3ca^{H1047R} or *Pten* deletion in the ovary induces serous papillary hyperplasia and together can cooperate to induce serous adenocarcinomas or granulosa cell tumors

Histology by genotype	Frequency
Pik3ca^{WT}*Pten*$^{+/+}$	
Normal	6/6 (100%)
Pik3ca^{WT}*Pten*$^{del/+}$	
Normal	3/3 (100%)
Pik3ca^{WT}*Pten*$^{del/del}$	
Normal	1/6 (16.7%)[A]
SPH grade 1	5/6 (83.3%)
Pik3ca^{H1047R}*Pten*$^{+/+}$	
Normal	1/5 (20%)
SPH grade 1	1/5 (20%)
SPH grade 2	1/5 (20%)
SPH grade 3	2/5 (40%)
Pik3ca^{H1047R}*Pten*$^{del/+}$	
SPH grade 1	1/5 (20%)
SPH grade 2	3/5 (60%)
SPH grade 3	1/5 (20%)
Pik3ca^{H1047R}*Pten*$^{del/del}$ [B]	
Serous adenocarcinoma	10/15 (67%)
Granulosa cell tumor	7/15 (46%)
Luteoma	1/15 (6.6%)
Endometriosis-like hemorrhage	4/15 (27%)

[A]One mouse was sacrificed due to illness at 14 weeks (unknown cause); ovaries were described as normal. [B]Collision tumors (both serous and granulosa cell histopathology) were observed in 3 mice. SPH, serous papillary hyperplasia. Mice were analyzed at 45–52 weeks after AdCre infection, except for the *Pik3ca*^{H1047R}*Pten*$^{del/del}$ group, which were sacrificed at 9–28 weeks after AdCre infection due to illness.

Statistics. Statistical analyses were performed using a 2-tailed Student's *t* test or log-rank (Mantel-Cox) Kaplan-Meier survival test. *P* values less than 0.05 were considered statistically significant.

Study approval. Animal experiments followed the National Health and Medical Research Council (NHMRC) Australian Code of Practice for the Care and Use of Animals for Scientific Purposes and were approved by the PMCC ethics committee.

Acknowledgments

We thank Kerry Ardley for animal experiments and the Peter Mac core histology and pathology facilities. This work was supported by the NHMRC (grant no. 628620 to W.A. Phillips and no. 566876 to G.A. McArthur and R.B. Pearson); the Association of International Cancer Research (no. 10-0052 to W.A. Phillips); Pfizer (grant to G.A. McArthur and R.J. Hicks); the Cancer Council Victoria and the Victorian Cancer Agency (grants to R.W. Johnstone); and the Victorian Breast Cancer Research Consortium, Australia (to I.G. Campbell and K.L. Gorringe). Researchers were funded by a Sir Edward Weary Dunlop Fellowship, Cancer Council of Victoria (to G.A. McArthur); research fellowships from the NHMRC (to R.B. Pearson and R.W. Johnstone); Cure Cancer Australia Foundation and Cancer Australia (to I. Ivetac); the Egyptian government and NHMRC (to M. Saad); Australian Postgraduate Research Awards (to L. Hare and G.L. Ryland); and the Swiss National Science Foundation (to V. Roh).

Received for publication June 7, 2011, and accepted in revised form November 16, 2011.

Address correspondence to: Wayne A. Phillips, Surgical Oncology Research Laboratory, Research Division, Peter MacCallum Cancer Centre, Locked Bag 1, A'Beckett Street, Melbourne, VIC 8006, Australia. Phone: 61.3.96561842; Fax: 61.3.96561411; E-mail: wayne.phillips@petermac.org.

1. Campbell IG, et al. Mutation of the PIK3CA gene in ovarian and breast cancer. *Cancer Res*. 2004; 64(21):7678–7681.
2. Samuels Y, et al. High frequency of mutations of the PIK3CA gene in human cancers. *Science*. 2004; 304(5670):554.
3. Zhao L, Vogt PK. Class I PI3K in oncogenic cellular transformation. *Oncogene*. 2008;27(41):5486–5496.
4. Altomare DA, et al. AKT and mTOR phosphorylation is frequently detected in ovarian cancer and can be targeted to disrupt ovarian tumor cell growth. *Oncogene*. 2004;23(34):5853–5857.
5. Bast RC, Hennessy B, Mills GB. The biology of ovarian cancer: new opportunities for translation. *Nat Rev Cancer*. 2009;9(6):415–428.
6. Despierre E, Lambrechts D, Neven P, Amant F, Lambrechts S, Vergote I. The molecular genetic basis of ovarian cancer and its roadmap towards a better treatment. *Gynecol Oncol*. 2010;117(2):358–365.
7. Gorringe KL, Campbell IG. Large-scale genomic analysis of ovarian carcinomas. *Mol Oncol*. 2009; 3(2):157–164.
8. Shayesteh L, et al. PIK3CA is implicated as an oncogene in ovarian cancer. *Nat Genet*. 1999;21(1):99–102.
9. Hashiguchi Y, Tsuda H, Inoue T, Berkowitz RS, Mok SC. PTEN expression in clear cell adenocarcinoma of the ovary. *Gynecol Oncol*. 2006;101(1):71–75.
10. Ramakrishna M, et al. Identification of candidate growth promoting genes in ovarian cancer through integrated copy number and expression analysis. *PLoS One*. 2010;5(4):e9983.
11. Wu R, et al. Mouse model of human ovarian endometrioid adenocarcinoma based on somatic defects in the Wnt/beta-catenin and PI3K/Pten signaling pathways. *Cancer Cell*. 2007;11(4):321–333.
12. Dinulescu DM, Ince TA, Quade BJ, Shafer SA, Crowley D, Jacks T. Role of K-ras and Pten in the development of mouse models of endometriosis and endometrioid ovarian cancer. *Nat Med*. 2005;11(1):63–70.
13. Liang S, et al. Expression of activated PIK3CA in ovarian surface epithelium results in hyperplasia but not tumor formation. *PLoS One*. 2009;4(1):e4295.
14. Rodriguez-Viciana P, et al. Role of phosphoinositide 3-OH kinase in cell transformation and control of the actin cytoskeleton by Ras. *Cell*. 1997;89(3):457–467.
15. Gupta S, et al. Binding of ras to phosphoinositide 3-kinase p110alpha is required for ras-driven tumorigenesis in mice. *Cell*. 2007;129(5):957–968.
16. Yuan TL, Cantley LC. PI3K pathway alterations in cancer: variations on a theme. *Oncogene*. 2008;27(41):5497–5510.
17. Groszer M, et al. Negative regulation of neural stem/progenitor cell proliferation by the Pten tumor suppressor gene in vivo. *Science*. 2001; 294(5549):2186–2189.
18. Flesken-Nikitin A, Choi K-C, Eng JP, Shmidt EN, Nikitin AY. Induction of carcinogenesis by concurrent inactivation of p53 and Rb1 in the mouse ovarian surface epithelium. *Cancer Res*. 2003; 63(13):3459–3463.
19. Clark-Knowles KV, Senterman MK, Collins O, Vanderhyden BC. Conditional inactivation of Brca1, p53 and Rb in mouse ovaries results in the development of leiomyosarcomas. *PLoS One*. 2009;4(12):e8534.
20. Engelman JA, et al. Effective use of PI3K and MEK inhibitors to treat mutant Kras G12D and PIK3CA H1047R murine lung cancers. *Nat Med*. 2008; 14(12):1351–1356.
21. Adams JR, et al. Cooperation between Pik3ca and p53 mutations in mouse mammary tumor formation. *Cancer Res*. 2011;71(7):2706–2717.
22. Meyer DS, Brinkhaus H, Muller U, Muller M, Cardiff RD, Bentires-Alj M. Luminal expression of PIK3CA mutant H1047R in the mammary gland induces heterogeneous tumors. *Cancer Res*. 2011;71(13):4344–4351.
23. Liu P, et al. Oncogenic PIK3CA-driven mammary tumors frequently recur via PI3K pathway-dependent and PI3K pathway-independent mechanisms. *Nat Med*. 2011;17(9):1116–1120.
24. Cancer Genome Atlas Research Network. Integrated genomic analyses of ovarian carcinoma. *Nature*. 2011;474(7353):609–615.
25. Zhang S, Yu D. PI(3)King apart PTEN's role in cancer. *Clin Cancer Res*. 2010;16(17):4325–4330.
26. Cheng H, et al. Discovery of the highly potent PI3K-mTOR dual inhibitor PF-04691502 through structure based drug design. *MedChemComm*. 2010;1:139–144.
27. Kinross KM, et al. In vivo activity of combined PI3K/mTOR and MEK inhibition in a Kras(G12D);Pten deletion mouse model of ovarian cancer. *Mol Cancer Ther*. 2011;10(8):1440–1449.
28. Shibata H, et al. Rapid colorectal adenoma formation initiated by conditional targeting of the *Apc* gene. *Science*. 1997;278(5335):120–123.
29. Jackson EL, et al. Analysis of lung tumor initiation and progression using conditional expression of oncogenic K-ras. *Genes Dev*. 2001;15(24):3243–3248.